Micromechanical torque magnetometer with sub-monolayer sensitivity ☆

D.H. Min[a,b,*], A. McCallum[a], Stephen E. Russek[a], John Moreland[a]

[a]National Institute of Standards and Technology, Boulder, CO 80305, USA
[b]Colorado School of Mines, Golden, CO 80401, USA

Abstract

We have developed a micromechanical torque sensor with sub-monolayer sensitivity for in situ monitoring of the magnetic moment of thin films during deposition. The film is deposited onto a microcantilever. The torque on the film is determined by measuring the deflection of the cantilever due to a small AC magnetic field perpendicular to the surface of the film. The microcantilevers have a high mechanical quality factor, large surface area, low spring constant, and high resonance frequency to improve film sensitivity to thickness. A phase-locked loop minimizes the resonance frequency shift of the cantilever due to mass loading and temperature drift that would otherwise affect the measurement of magnetic torque. The demonstrated thickness sensitivity for a $Ni_{0.8}Fe_{0.2}$ film and a $Ni_{0.8}Fe_{0.2}/Cu$ multilayer film is less than 0.1 nm.
© 2004 Elsevier B.V. All rights reserved.

1. Introduction

This paper describes a new technique for sensing the small changes in magnetic moment of ferromagnetic films as each monolayer is deposited. Magnetic film properties are usually determined ex situ, since implementing conventional magnetometer sensors in high-vacuum or ultra-high-vacuum (UHV) environments is difficult. There are several reasons for developing in situ magnetometry: (1) measurements of the magnetic moment of a thin film during its deposition is desirable in order to avoid any degradation of its properties caused by possible oxidation after breaking a vacuum; (2) a fundamental understanding of interlayer coupling and interlayer mixing mechanisms can be achieved; (3) real-time

---

☆Contribution of the National Institute of Standards and Technology, not subject to copyright.

*Corresponding author.

E-mail address: dhmin@boulder.nist.gov (D.H. Min).

monitoring of the magnetic moments of thin films during the film deposition becomes a cost-effective possibility.

2. Operating principles

Our approach is based on a micromechanical cantilever sensor customized for thin-film magnetometry. The cantilever consists of a rectangular beam "spring" attached to a "paddle" substrate. The film is deposited directly onto the paddle. A small AC field H_t applied perpendicular to the surface of the film causes the spring to vibrate. If the energy stored in the spring cantilever is sufficiently small, compared to the anisotropy energy, then the deflection of the spring is proportional to the magnetic moment of the film [1]. The dimensions of the microresonator are shown in Fig. 1(a). The field orientations and torque directions are shown in Fig. 1(b). Fig. 1(c) shows the setup for a resonating torque magnetometer. Two samarium–cobalt permanent magnets generate the bias field H_0, and a small

Fig. 1. A micromechanical torque magnetometer: (a) dimensions of cantilever spring and paddle; (b) torque direction due to a saturation magnetization M_s crossed into the AC torque field H_t; (c) setup diagram of cantilever operation.

solenoid generates a perpendicular torque field H_t. Simple beam bending formula gives the displacement of cantilever [2]:

$$Z = \frac{6T_M l_c^2}{E w_c t_c^3},$$

where w_c is the cantilever width, E is Young's modulus, l_c is the cantilever length, t_c is the cantilever thickness, and $T_M = \mu_0 V_f M_s H_t$, assuming that the torque on the film acts as a bending moment concentrated at the end of the beam. In the expression for T_M, V_f is the volume of a film and M_s is the saturation magnetization of a film. We measured the bias field H_0 profile near the center, where the paddle ($1\,\text{mm} \times 1\,\text{mm}$) is located, and found the field to be uniform at $23.8\,\text{kA/m}$ within $\pm 1\,\text{mm}$ from the center. Within $\pm 2\,\text{mm}$ from the center, the field was $25.0\,\text{kA/m}$, which is different by $\sim 5\%$ compared to the field at the center. The AC magnetic torque field was $H_t = 300\,\text{A/m}$.

The Q value was measured by free decay of the vibration of the beam and found to be 1.050×10^5. The theoretical resonance frequency f_0, based on a distributed mass model [3] of a silicon paddle cantilever with dimensions shown in Fig. 1(a), is $3.783\,\text{kHz}$, which is close to our measured range of 3.956–$4.020\,\text{kHz}$ for a 5 nm thick $Ni_{0.8}Fe_{0.2}$ deposited film. The spring constant is approximately $0.055\,\text{N/m}$, based on the cantilever spring dimensions and the modulus of silicon. Given these parameters, the cantilever thermal fluctuations in a 1 Hz bandwidth are

$$Z_{\text{thermal}} = \sqrt{\frac{2k_B T}{\pi Q K_s f_0}},$$

where $K_s = E w_c t_c^3 / 6 l_c^3$ is the spring constant [4]. We can, therefore, predict the ultimate signal-to-noise ratio (SNR) for this setup with a 1 Hz bandwidth [5] as

$$\text{SNR}_{\text{thermal}} = \frac{Z}{Z_{\text{thermal}}} = 6 \frac{T_M}{l_c} \sqrt{\frac{\pi Q f_0}{2 K_s k_B T}},$$

where Q is the mechanical quality factor, $k_B T$ is the thermal energy, k_B is Boltzmann's constants, and T_M is the torque due to the magnetic film. Theoretically, we calculate $Z = 2.27 \times 10^{-13}\,\text{m}$,

$Z_{\text{thermal}} = 1.13 \times 10^{-16}$ m, and $\text{SNR}_{\text{thermal}} = 2.01 \times 10^{3}$ for a 0.1 nm thick $Ni_{0.8}Fe_{0.2}$ film, using the measured saturation magnetization $M_s = 6.8 \times 10^{5}$ A/m for a thin film. We found experimentally that the $\text{SNR} = 1.1$ for a 0.1 nm-thick $Ni_{0.8}Fe_{0.2}$ film during the deposition with deposition rate 0.078 nm/s. The lock-in amplifier integration constant was set to 100 ms well below the 500 ms time period between data points. The noise is probably due to the vibrations of the UHV system. Note that even if vibration could be minimized, the instrument would still be limited by the optic fiber interferrometer sensitivity $Z_{\text{fiber}} = 1.36 \times 10^{-15}$ m/$\sqrt{Hz}$, and $\text{SNR}_{\text{fiber}} = Z/Z_{\text{fiber}} = 166$ for a 0.1 nm $Ni_{0.8}Fe_{0.2}$ film.

3. Experimental setup

An 8 nm-thick $Ni_{0.8}Fe_{0.2}$ film was deposited on the opposite side of the grooved surface of the paddle. This was necessary in order to find the resonance torque frequency of the cantilever so that the magnetometer can be tuned before deposition. The experimental setup for this specific application is shown in Fig. 2(a). The oscillator chip was mounted in a deposition head (Fig. 2(b)) with the cantilever paddle located between the two SmCo magnets. An optical fiber interferometer (single mode, fiber core: 5 μm), similar to the conventional optical fiber interferometers developed for atomic force microscopy (AFM) [6], was used to measure the cantilever's deflection. A fraction of the laser light (~4%) passing through a directional coupler is reflected by the fiber facet, and the remainder is reflected by the cantilever paddle surface. These beams interfere with each other and form a single reflected beam that travels back through the fiber and is detected as an output signal by the photodetector. A laser diode is controlled by a diode driver, and the wavelength is changed by the laser temperature to be on the steep part of the interference fringe [7]. A phase detector measures the phase difference between the output signal from the interferometer and the signal input to the coil that generates torque field H_t. A proportional-integral-differential (PID) controller and a voltage-controlled oscillator (VCO)
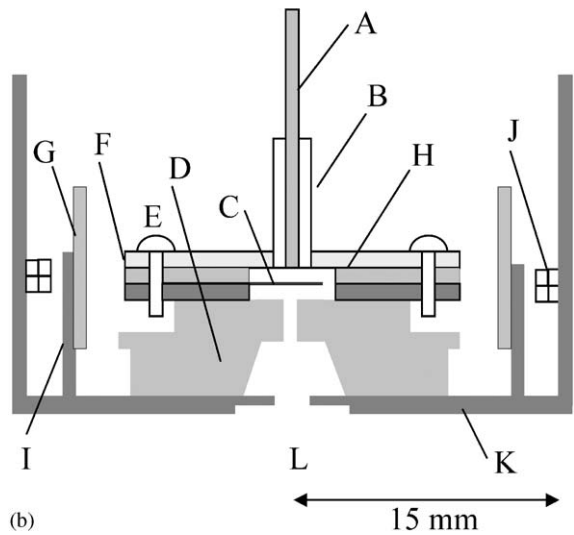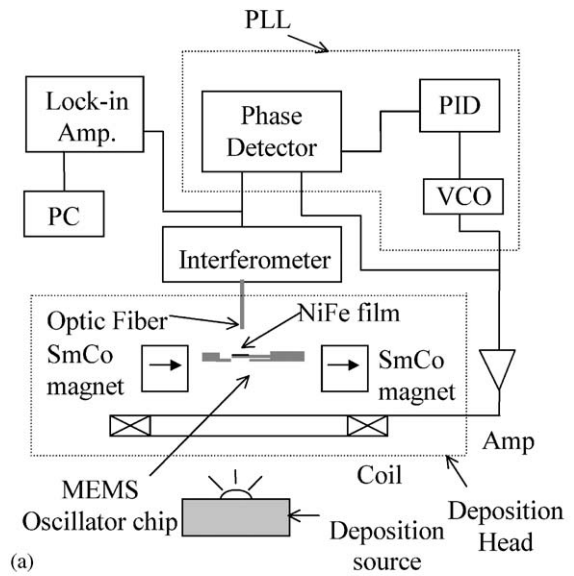
Fig. 2. Schematic diagram of experimental setup: (a) components of a resonating torque magnetometer; (b) Cross-sectional diagram of deposition head where A: fiber core (5 μm diameter); B: clad; C: oscillator chip; D: ceramic material; E: screw; F: fiber optic part; G: SmCo permanent magnet; H: SU8 photoresist; I: copper support for SmCo magnet; J: coil; K: deposition shield; L: deposition hole.

keep the phase difference the same as the value set in the PID controller. The phase detector, the PID controller, and the VCO make up the phase-locked

loop (PLL), which tracks the shifts in resonance frequency due to the mass-loading effect and thermal drift during the film deposition. The instrument, therefore, provides a signal proportional to the magnetic signal, separate from the effects of mass loading and thermal drift.

4. Fabrication of oscillator chips

At the heart of this magnetometer design is a silicon oscillator chip fabricated from a double-sided polished $\langle 1 0 0 \rangle$-oriented single-crystal silicon wafer of which the diameter and thickness are 75 mm and 350 μm, respectively. Fig. 3 shows the diagram of the oscillator chip assembly, which consists of two parts. One is a cantilever paddle (Fig. 3(a)) and the other is a deposition mask (Fig. 3(b)) that is used to ensure that the film is deposited only on the paddle. If the magnetic film were deposited onto the cantilever, the signal would not be proportional to the magnetic moment of the deposited film due to the reduction in Q [8]. The deposition mask has a square hole
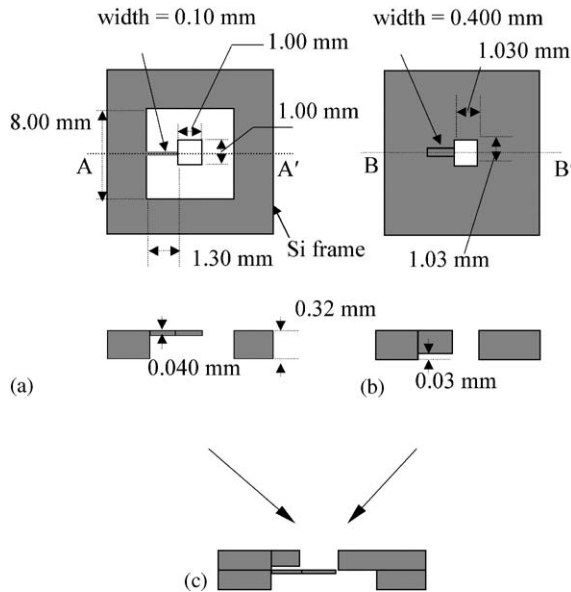
Fig. 3. Schematic diagram of oscillator chip: (a) cantilever paddle and its cross section; (b) deposition mask and its cross section; (c) the cross-sectional view of oscillator chip assembly.
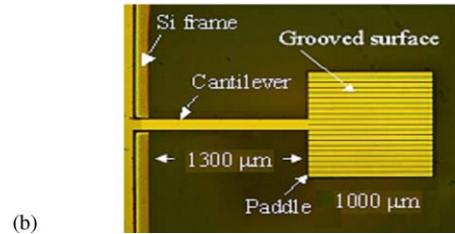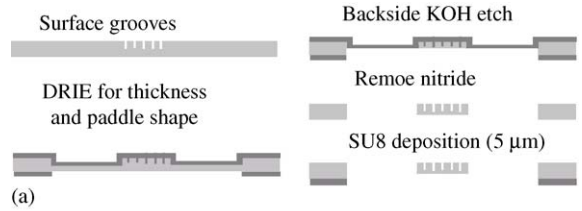
Fig. 4. Diagram of cantilever paddle process steps: (a) the fabrication process steps of the cantilever paddle with SU8 spacer; (b) the photograph of finished paddle cantilever.

slightly larger than the paddle dimensions. The surface of the paddle is grooved (width 5 μm, depth 4 μm, period 50 μm) to minimize the eddy-current effect that may possibly reduce the output signal slightly [9]. These two parts are bonded together as shown in Fig. 3(c). Details of the chip fabrication process are shown in Fig. 4(a). First, we started with a buffered oxide etch (BOE) to remove the oxide from the silicon wafer. Then we made grooves in the cantilever paddle using several steps of lithography and deep reactive ion etching (DRIE). A cantilever thickness of 40 μm was determined by timing the DRIE process. Second, we deposited 0.4 μm Si_3N_4 on both sides of the wafer and the backside nitride was then patterned using reactive ion etching (RIE). The cantilever release process is based on a KOH anisotropic etch (30% by weight with 2–3% of isopropyl alcohol (IPA), and an oxygen bubbler at 75 °C) through a silicon wafer with a lithographically patterned layer of Si_3Ni_4 as a wet etch mask in the KOH solution. After the KOH etch, the Si_3Ni_4 layer on the front side was removed before magnetic film deposition. The roughness of the paddle surface is important because it will influence the magnetic properties of the deposited film. In particular, the anisotropy of the film can be strongly related to the substrate roughness.

R_rms = 0.263 nm   R_rms = 0.313 nm

0.3 μm   0.3 μm

(a)   (b)

R_rms = 0.898 nm   R_rms = 1.14 nm

0.3 μm   0.3 μm

(c)   (d)
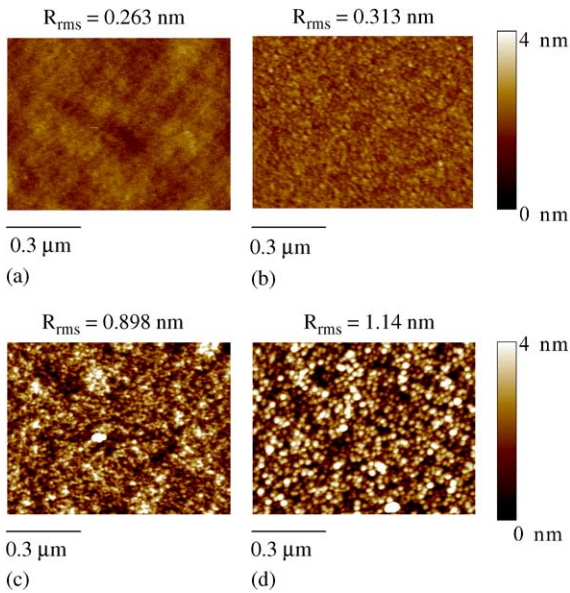
Fig. 5. AFM images of (a) unprocessed bare Si surface; (b) surface of 5 nm NiFe film on the bare Si surface; (c) paddle surface after the nitride film is removed by RIE; and (d) surface of 5 nm NiFe film on the paddle.

Fig. 5 shows atomic-force microscope (AFM) images of the paddle surface before and after the deposition of the 5 nm $Ni_{0.8}Fe_{0.2}$ film. The rms surface roughness R_{rms} was 0.89 nm for the paddle before the film deposition, and 1.11 nm after the film deposition, compared to a surface roughness 0.26 nm of unprocessed silicon and 0.31 nm for a 5 nm of $Ni_{0.8}Fe_{0.2}$ deposited on unprocessed silicon. According to the AFM images of the $Ni_{0.8}Fe_{0.2}$ on the paddle, after nitride processing, we found that the substrate tilt considering long-range surface roughness over a few micrometers is less than 3°. This is probably not a major source of anisotropy and can be neglected. However, the short-range roughness of the $Ni_{0.8}Fe_{0.2}$ film, after nitride processing is not negligible compared to similar films on the unprocessed wafers. We are carefully developing fabrication steps to improve cantilever roughness in order to address this issue.

Once the nitride had been removed, 5 μm of SU8 [10] photoresist were spun onto only the silicon frame surrounding the cantilever paddle. The SU8 acts as a spacer to fix the distance between the fiber end and the paddle surface in the final assembly. In order to eliminate the need for wafer dicing, the cantilever frame is connected to the rest of the wafer by break-off tabs, shown in Fig. 3(a). The finished cantilever is shown in Fig. 4(b).

Once the oscillator chips were fabricated, they were mounted in the deposition head, as shown in Fig. 2(b). The cleaved end of the optical fiber is set above the cantilever at a distance that is determined by the thickness of the SU8 photoresist. The detailed process for SU8 can be found in Ref. [11].

5. Measurements of deposition of thin films

Magnetron sputter-gun deposition sources were used to deposit multilayer films of $Ni_{0.8}Fe_{0.2}$, and $Ni_{0.8}Fe_{0.2}$/Cu onto the cantilever paddle. Depositions were done in an ultra-high-vacuum chamber with a base pressure of 2.6×10^{-6} Pa that is routinely obtained after a 100 °C bake-out for 12 h. During the deposition, the background pressure was 1×10^{-5} Pa of argon. The magnetic moments of multilayer films of $Ni_{0.8}Fe_{0.2}$ and $Ni_{0.8}Fe_{0.2}$/Cu were measured, as a function of film thickness, during the deposition. The film thickness was determined with a commercial quartz-crystal thickness monitor within an uncertainty of 0.1 nm. The films were deposited with a deposition rate ranging from 0.17 to 0.18 nm/s for $Ni_{0.8}Fe_{0.2}$ and ∼0.088 nm/s for Cu film. Fig. 6(a) shows the graph of the output signal vs. thickness for deposition of 5 nm $Ni_{0.8}Fe_{0.2}$. As shown in the graph, the magnetic signal does not increase up to film thicknesses around 1.4 nm, indicating that magnetically "dead" layers are created at the very beginning stage of deposition. The measured dead layer (∼4 monolayers) is somewhat thick compared to experiments on multilayers grown on single crystal substrates that become magnetic after two monolayers. It is probably due to the nucleation stages of the film growth and the formation of silicides at the interface between the silicon paddle substrate and the metallic film. In principle, buffer layers could be predeposited and annealed in UHV prior to the deposition of a magnetic multilayer to improve the surface

(a)

(b)
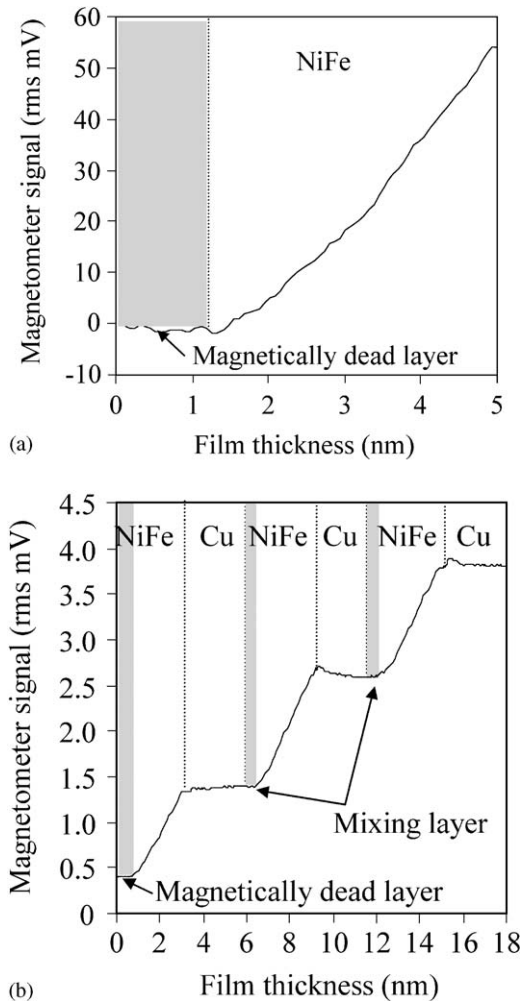
Fig. 6. Magnetometer response as a function of film thickness measured with a quartz crystal micro-balance (QCMB) for $Ni_{0.8}Fe_{0.2}$ (5 nm) and $Ni_{0.8}Fe_{0.2}$ (3 nm)/Cu (3 nm) multilayer films.

roughness and crystallographic properties of the paddle substrate. Alternatively, a thin (less than 100 μm) polished single crystal wafer patterned using a laser a cutting tool could be bonded to the silicon paddle surface using wafer level assembly techniques (flip-chip bonding for example) before the cantilevers are released form the wafer. For film thicknesses greater than 1.4 nm, the magnetic signal increases with thickness of $Ni_{0.8}Fe_{0.2}$. The monitoring result of a multilayer of $Ni_{0.8}Fe_{0.2}$/Cu is shown in Fig. 6(b). The magnetically dead layers were also found at the beginning of the film growth of the first layer of $Ni_{0.8}Fe_{0.2}$. The magnetic signal increases with deposition of $Ni_{0.8}Fe_{0.2}$ after ~1 nm, and the signal stays constant during the deposition of copper before increasing again with another deposition of $Ni_{0.8}Fe_{0.2}$. We believe that the magnetic signal at the interface between Cu and $Ni_{0.8}Fe_{0.2}$ does not correspond to a sharp transition because there is some intermixing between the Cu and $Ni_{0.8}Fe_{0.2}$. We estimate the thickness of the first and second intermixing regions to be about 0.5 and 0.9 nm, respectively, based on the data in Fig. 6(b).

In summary, we have developed an instrument for monitoring the magnetic moment of thin films and multilayers with submonolayer sensitivity, during film deposition. This instrument combines custom micromachined mechanical torque sensors with an interferometer similar to that developed for atomic force microscopy to achieve unprecedented sensitivity to magnetic thickness at room temperature. Our results show that this instrument has promise for the study of magnetic interlayer coupling mechanisms such as Ruderman–Kittel–Kasuya–Yosida (RKKY) and superexchange of thin magnetic films [12–14].

References

[1] M. Lohndof, J. Moreland, P. Kabos, Appl. Phys. Lett. 76 (2000) 1176–1178.
[2] R.J. Roark, W.C. Young, Formulas for Stress and Strain, fifth ed., McGraw-Hill, New Delhi, 1975, p. 105.
[3] U. Rabe, K. Janser, W. Arnold, Rev. Sci. Instrum. 67 (1996) 3281.
[4] W.T. Thomson, M.D. Dahleh, Theory of Vibration with Applications, fifth ed., Prentice-Hall Inc., Englewood Cliffs, 1998, p. 166.
[5] D. Sarid, Scanning Force Microscopy with Applications to Electric, Magnetic, and Atomic Forces, Oxford, New York, 1991, pp. 19–38.
[6] D. Rugar, H.J. Mamin, R. Erlandsson, J.E. Stern, B.D. Terris, Rev. Sci. Instrum. 59 (1988) 2337.
[7] J.A. Sidles, J.L. Garbini, K.J. Bruland, D. Rugar, O. Zuger, S. Hoen, C.S. Yannoni, Rev. Mod. Phys. 67 (1) (1995) 249–265.
[8] K. Lee, N. LaBianca, S. Rishton, S. Zohlgharnain, J. Vac. Sci. Technol. B 13 (1995) 3012–3016.

[9] M.H. Nayfeh, M.K. Brussel, Electricity and Magnetism, Wiley, New York, 1985, pp. 352–372.

[10] Trade name is stated for technical clarity and does not imply endorsement by NIST. Products from other manufacturers may perform as well or better.

[11] P. Lu, F. Shen, S.J. O'Shea, K.H. Lee, T.Y. Ng, Mater. Phys. Mech. 4 (2001) 51–55.

[12] M.A. Ruderman, C. Kittel, Phys. Rev. 96 (1954) 99.

[13] T. Kasuya, Prog. Theor. Phys. 16 (1956) 45.

[14] K. Yosida, Phys. Rev. 106 (1957) 893.